

Comparison Of Heat-Flux And Wall-Temperature Based Correlations For Predicting Post-Dryout Surface Temperature In Tubes

E.-L. Pelletier¹, L.K.H. Leung², R. Girard³, A. Teysedou¹ and E. Varin⁴

¹Engineering Physics Department, Ecole Polytechnique de Montréal,
Montréal, Québec H3T 1J4,

²Chalk River Laboratories, AECL, Chalk River, Ontario K0J 1J0

³Hydro Québec, Montréal, Québec,

⁴AECL, Montréal, Québec.

Abstract

Two correlations for predicting the post-dryout surface temperature have been assessed against a set of experimental data obtained in 12.6-mm inside diameter tubes of two different heated lengths. The first correlation for post-dryout heat-transfer coefficient is expressed in terms of the surface heat flux, while the second correlation is based on the wall superheat. These correlations consist of two components covering the fully developed post-dryout heat transfer and the developing post-dryout region. The fully developed post-dryout heat-transfer coefficient is evaluated from look-up tables, and the developing post-dryout heat transfer is expressed as modification factors that were derived from a large experimental database for tubes.

Wall-temperature distributions along these uniformly heated tubes were established using a semi-analytical scheme and compared against the measurements. Both correlations have been shown to provide good wall-temperature predictions. However, the overall prediction accuracy for the heat-flux-based correlation appears to be slightly better than that for the wall-superheat-based correlation. Furthermore, the heat-flux-based correlation follows closely the developing-post-dryout region as compared to the wall-superheat-based correlation.

1. Introduction

Surface temperature at fuel bundles is relatively low (i.e., close to the saturation temperature) during normal reactor operating conditions. Heat-transfer regimes encountered at these conditions are mainly single-phase forced convection to liquid, nucleate boiling, and forced convective evaporation. However, surface temperature may exceed the corresponding value at critical heat flux during postulated accidents, such as Loss-of-Flow Accident (LOFA) or Loss-of-Regulation Accident (LORA). The corresponding heat-transfer regime is referred as film boiling (or generally as the post-dryout heat-transfer mode). An increase in surface temperature has been observed experimentally in CANDU 37-element bundle simulator at post-dryout conditions. However, the increase is gradual and controllable with changes in flow conditions and power.

Reactor safety analysis codes, such as CATHENA, are applied in predicting surface-temperature variations in fuel bundles under postulated accident conditions. These codes calculate the local cross-sectional average thermalhydraulic conditions at any locations along

the fuel string, determine the associated heat-transfer mode and predict the surface temperature by using the appropriate heat-transfer correlation. Under some accident scenarios the thermalhydraulic conditions can vary quite rapidly and due to the large internal energy stored in the fuel during the transient, the surface heat flux is not correctly determined. Therefore, traditional correlations based on surface heat flux (since power is one of the independent experimental parameters) are cumbersome to be implemented. Wall-superheat-based correlations have recently been developed to circumvent the application issue of heat-flux-based correlations, and implemented into the CATHENA code for safety analyses [1]. Heat-flux-based correlations are still being applied in the subchannel codes for analysis of post-dryout characteristics in fuel bundles under steady-state conditions.

A systematic assessment of the prediction accuracy of the heat-flux-based and wall-superheat-based post-dryout correlation has been performed against surface-temperature measurements in tubes. The objective of this paper is to present the assessment result.

2. Post-Dryout Heat Transfer Model

The post-dryout heat-transfer coefficient in tubes is expressed as [2]:

$$h_{PDO} = K_{dev} h_{FD}, \quad (1)$$

where K_{dev} is the modification factor that takes into account developing-flow effect and h_{FD} is the post-dryout heat-transfer coefficient for the fully developed conditions. Additional modification factors, that are relevant for fuel-bundle analyses, have been introduced to account for other separate effects [2]. However, these factors are not applicable in the current study. Figure 1 illustrates the variation of the heat-transfer coefficient (and the corresponding surface temperature) in the developing and fully developed post-dryout regions [3].

Fully developed post-dryout conditions are considered once the vapour superheat is well established in the near-wall region, where it is assumed that the droplets can no longer impinge the heated surface. A large number of correlations and models have been developed for predicting the fully developed post-dryout heat-transfer coefficient. Groeneveld et al. [4] introduced the look-up table approach to improve the prediction accuracy and simplify the evaluation of the critical heat flux and the post-dryout heat transfer coefficient. Each look-up table tabulates discrete values established from a large experimental database over a wide range of flow conditions. A linear interpolation is applied for conditions within tabulated parameters. Two separate post-dryout look-up tables have been developed which present the fully developed post-dryout heat-transfer coefficient as a function of local flow conditions (i.e., pressure, mass flux and thermodynamic quality) for either the heat flux or the wall superheat.

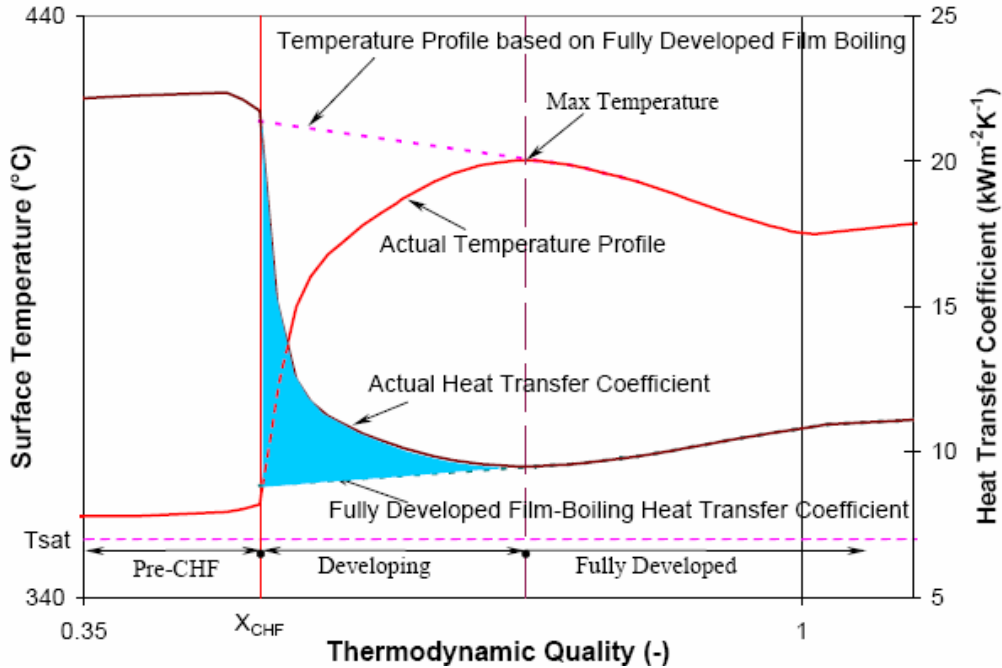


Figure 1: Evolution of the wall temperature and the heat transfer coefficient under CHF and post dryout conditions [3].

The developing post-dryout region corresponds to the evolution of the vapour superheat in the near-wall region. It is assumed that within this zone, the droplet impingement to the heated surface can occur. These possible droplet–wall interactions result in a relatively efficient heat-transfer rate between the heated surface and the coolant, as compared to the fully developed post-dryout flow (see Figure 1). Correlations that take into account the developing vapour-superheat effects have been written by using a large number of experimental data collected by using heated tubes. These correlations, based on either the heat flux or the wall superheat, are consistent with the selected look-up table approach. The heat-flux-based correlation for the developing-flow modification factor is expressed as [2]:

$$K_{dev} = 1 + \left(\frac{h_{nb}}{h_{FD}} - 1 \right) \exp \left[-a \left(\frac{x - x_{DO}}{(1 - x_{DO})Bo} \right)^b \right], \quad (2)$$

where the boiling number, Bo , is defined as

$$Bo = \frac{q}{GH_{fg}}. \quad (3)$$

The heat-transfer coefficient for nucleate boiling, h_{nb} , is calculated using the Chen correlation [5]. The dryout quality, x_{DO} , is determined at the local pressure, mass flux, and heat flux. The coefficients a and b are parameters obtained by fitting the experimental data of Becker et al. [6].

The modification factor for the wall-temperature-based correlation is expressed as [3]:

$$K_{dev} = 1 + \left(\frac{h_{nb}}{h_{FD}} \right) \exp[-c(WSR - 1)^b], \quad (4)$$

where the WSR ratio is defined as:

$$WSR = \frac{T_W - T_{sat}}{T_{CHF} - T_{sat}}. \quad (5)$$

In the above equation, T_{CHF} is defined as the wall temperature calculated with the local value of the CHF, the nucleate boiling heat transfer coefficient and the saturation temperature. Further, the nucleate boiling heat transfer coefficient is calculated by using Chen's forced convective boiling correlation with the local value of CHF as the heat flux.

The coefficients c and b are parameters obtained by fitting a large post-dryout surface temperature database [3].

3. Correlation assessment

The applicability of the heat-flux-based and wall-temperature-based post-dryout heat-transfer coefficients has been assessed against a set of experimental post-dryout surface-temperature measurements obtained in tubes of different heated lengths. Measurements obtained at fully developed conditions were used, together with other data sets, in the development of the heat-flux-based and wall-temperature-based look-up tables [4].

3.1 Experimental data

Bennett et al. [7] measured the surface temperature distributions in a vertical tube of 0.0127 m inside diameter. The tube was heated uniformly and cooled with an upward co-current flow of water at a pressure of 6893 kPa. Two heated-length values were used: 3.6576 m and 5.5626 m. The Figure 2 shows the schematic diagram of the test section with a 5.5626 m heated length. The surface temperatures were measured with thermocouples at various axial locations covering both pre-dryout and post-dryout conditions. A typical data set for different thermal powers is shown in Figure 3. Consistent with the temperature behaviour given in Figure 1, the Figure 3 shows a sharp surface temperature rise at the dryout point. This temperature rise, however, tends to stabilize after the dryout occurrence reaching a maximum value. Beyond this maximum temperature, the surface temperature decreases with increasing distance. It is assumed that within this region no direct liquid cooling is possible; thus, the film-boiling heat transfer has reached fully developed conditions. Developing film-boiling conditions are assumed between the dryout point and the maximum surface temperature location. The decrease in the surface temperature observed in the fully developed region is mainly caused by an increase of the forced-convective heat-transfer rate due to the increase of the flow velocity with quality. On the other hand, the increase in surface temperature in the developing film-boiling region is mainly caused by the gradual reduction in the wall droplet-impingement rate with increasing the quality.

For all the thermal powers applied during the experiments, the wall temperatures at the outlet of the test converge to almost the same value.

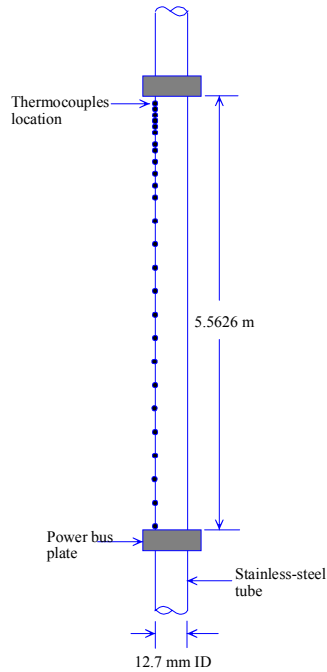


Figure 2: Schematic diagram of the test section [6].

The assessment presented in this paper is based on relatively high-flow rates (i.e., mass fluxes greater than $1000 \text{ kg/m}^2\text{s}$) obtained with the test section having a heated length of 5.56-m. A total of 702 post-dryout measurements taken from 104 test runs, including both developing and fully developed film-boiling regimes, have been treated. The following range of flow conditions is covered:

Channel Outlet Pressure	: 6.893 MPa (constant)
Mass Flux	: 1003 to 5235 $\text{kg/m}^2\text{s}$
Heat Flux	: 667 to 2086 kW/m^2
Inlet Fluid Temperature	: 259 to 276 $^{\circ}\text{C}$

3.2 Model description and simplifications

For given thermal power and experimental flow conditions, a semi-analytical steady-state calculation scheme is used for determining the wall-temperature distribution along the heated tube. The critical heat flux and the nucleate or film boiling heat transfer coefficients are determined depending on the difference between the local and critical heat fluxes at each experimental thermocouple location. The post-dryout heat-transfer coefficient is calculated using either the heat-flux-based or the wall-temperature-based methodology.

The application of the heat-flux-based methodology for predicting the post-dryout surface temperature is rather straightforward because the heat flux is calculated from the applied

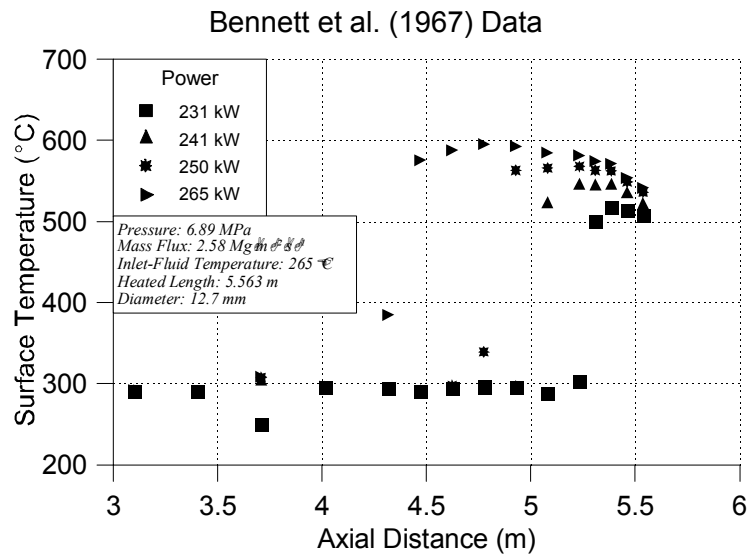


Figure 3: Surface temperature measurements [6].

power and the heated surface area. The post-dryout heat-transfer coefficient is calculated using Equation (2) and the post-dryout heat-transfer look-up table based on the local flow conditions and the experimental heat flux. The local wall temperature is calculated with:

$$T_w = \frac{q}{h_{PDO}} + T_{bulk} \quad (6)$$

In turn, the application of the wall-temperature-based methodology is more cumbersome because the wall temperature is a measured parameter. Therefore, an iterative approach is used to evaluate the post-dryout heat-transfer coefficient by using Equation (4) and the wall-temperature-based post-dryout heat-transfer look-up table. This iterative scheme is briefly shown in Figure 4.

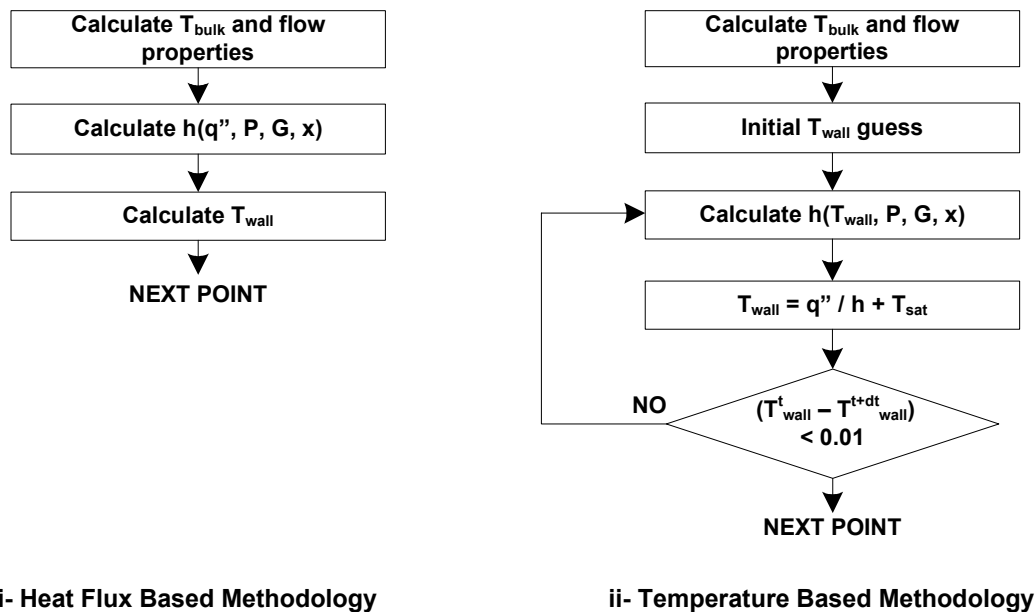


Figure 4. Heat transfer calculation schemes.

The critical heat flux has a strong impact on the prediction accuracy of the post-dryout heat transfer, particularly in the developing-flow region. A slight deviation in the predicted dryout location can result in a significant underprediction (or overprediction) of the post-dryout surface temperature (see Figure 3). Since this study is focused on the prediction accuracy of post-dryout surface temperature, a correction is applied to eliminate any systematic bias in the predicted critical heat flux as compared to the experimental value. In this study, the critical heat flux is predicted using the CHF look-up table for tubes [8]. The bias of the look-up table is determined for each test (i.e., under similar inlet flow temperature, mass flow rate and outlet pressure). Further, since the look-up table presents correct parametric trends and no significant fluctuations are observed among tabulated values, this bias is assumed systematic. The same bias (or correction factor) is applied to all post-dryout calculations within the same test run.

4. Assessment results

Post-dryout wall temperatures have been predicted using either the heat-flux-based or the wall-temperature-based correlations and compared against data of Bennett et al. [7] for various axial locations. Table 1 presents the prediction accuracy of these correlations for both developing and fully developed post-dryout regions. The prediction error is estimated as:

$$Avg. Error = \frac{1}{n} \sum_{i=1}^n Error_i, \quad (7)$$

where

$$Error = \frac{\text{predicted wall temperature}}{\text{measured wall temperature}} - 1. \quad (8)$$

The standard deviation is defined as:

$$Std. Dev. = \sqrt{\frac{1}{n-1} \sum_{i=1}^n (Error_i - Avg. Error)^2}. \quad (9)$$

Table 1: Assessment errors and standard deviations

		Correlation	
		Heat-Flux-Based	Wall-Temperature-Based
Developing Flow Region	Avg. Error (%)	-4.4	8.3
	Std. Dev. (%)	14.3	10.7
Fully Developed Flow Region	Avg. Error (%)	-0.8	1.8
	Std. Dev. (%)	8.6	6.4
All Regions	Avg. Error (%)	-2.1	4.2
	Std. Dev. (%)	11.2	8.8
Maximum Wall Temperature	Avg. Error (%)	-0.8	3.4
	Std. Dev. (%)	8.6	6.9

The experimental maximum wall temperature is used to separate the developing and the fully developed post-dryout regions. As shown in Figure 1, a fully developed post-dryout temperature is considered at positions downstream of the maximum temperature point. Otherwise, a developing flow temperature is assumed. The total 702 data points are then classified in each post-dryout region; 441 points are in fully developed conditions and 261 in developing flow conditions.

4.1 Heat-flux based methodology

The heat-flux-based method provides accurate wall-temperature prediction in the fully developed region with an average error of -0.8% and a standard deviation of 8.6%. However, it underpredicts the wall temperature in the developing-flow region with an average error of -4.4% and a standard deviation of 14.6%. The relatively large prediction error observed for the developing flow region is mainly due to the sharp wall temperature excursion occurring when dryout is encountered. The heat-flux-based correlation, however, exhibits a smaller rise in temperature than the measured value. Despite the underprediction, the maximum wall temperature along the tube is predicted with an accuracy of -0.8% and a standard deviation of 8.6%.

The predicted surface temperatures are compared with the experimental data in the Figure 5. In general, the predicted surface-temperature distribution using the heat-flux-based correlation follows closely the experimental trend. The heat-flux-based correlation predicts the surface-temperature with an average error of -2% and a standard deviation of 11% over the complete post-dryout region.

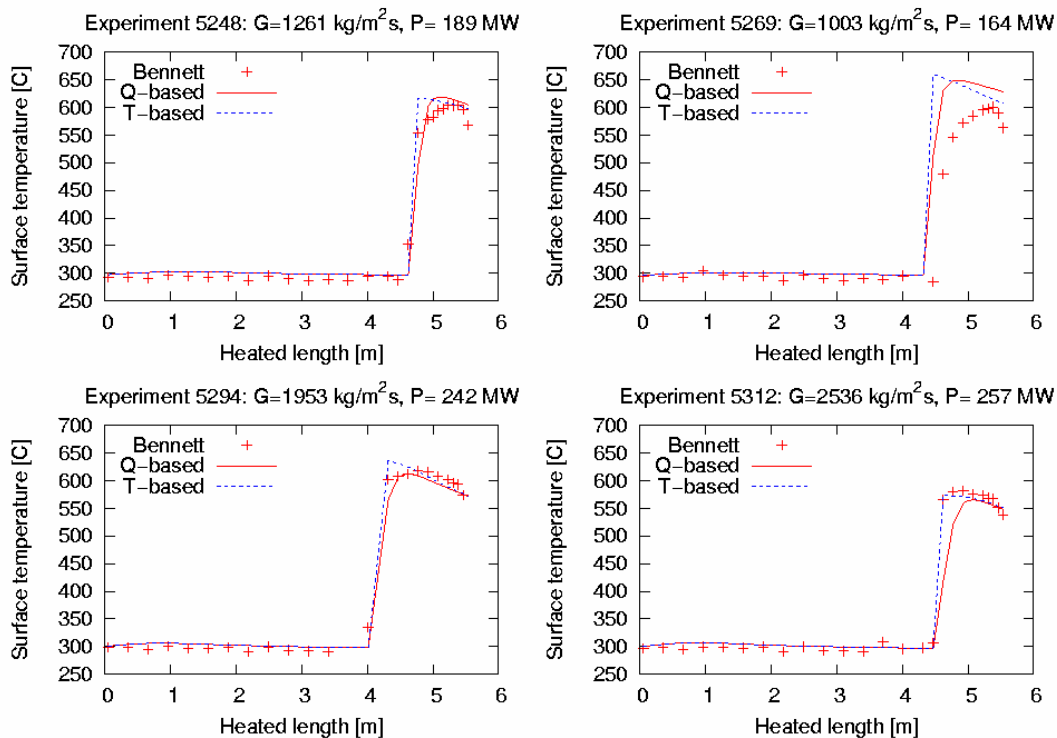


Figure 5: Experimental and calculated wall temperature distribution for typical cases

4.2 Temperature based methodology

The surface-temperature-based correlation predicts the wall temperature in the fully developed region with an average error of 1.8% and a standard deviation of 6.4%. Unlike the heat-flux-based correlation, it tends to over predict the wall temperature in the developing flow region with an average error of 8.3% and a standard deviation of 10.6%. This is the result of a much more rapid rise in the predicted surface temperature than the experimental trend when dryout occurs. As illustrated in Figure 5, the surface temperature approaches the fully developed value at

locations just downstream of the dryout point, i.e., the developing-flow region is very short or it is not present at all. By combining the two regions of post-dryout heat transfer, the wall-temperature-based correlation overpredicts wall-temperature with an average error of 4.2% and a standard deviation of 8.8%. Furthermore, the sharp temperature excursion has led to over predictions of the maximum wall temperature along the tube; the average error is 3.4% with a standard deviation of 6.9%.

As described in Section 2, the evaluation of the post-dryout heat-transfer coefficient using the wall-temperature-based correlation requires an iterative procedure based on an initial estimation of the wall temperature. A sensitivity analysis has been performed using various initial estimates and it has shown a negligible impact on the predicted post-dryout heat-transfer coefficient.

4.3 Sensitivity Assessment of the developing-flow modification factor

The prediction accuracy of the post-dryout surface temperature strongly depends on the developing-flow modification factor in either the heat-flux-based or the wall-temperature-based correlation. An underprediction of the surface temperature for the heat-flux-based correlation can be attributed to the relatively smooth variation of the developing-flow factor after the CHF occurrence. Contrarily, the overprediction of the surface temperature for the wall-temperature-based correlation is caused by a sharp change of the developing-flow modification factor. Therefore, a sensitivity analysis of this factor on the predicted wall temperature has been performed.

Figure 6(i) shows the impact of a $\pm 10\%$ change in the developing-flow modification factor for the two correlations. An increase in the developing-flow modification factor tends to reduce the predicted wall-temperature error. The wall-temperature prediction is very sensitive to the wall-temperature-based modification factor. A $\pm 10\%$ change in the developing-flow modification factor has led to about 20% change in the predicted wall-temperature error. The variation in the heat-flux-based factor on the other hand has only a small impact on the prediction (i.e., the error is less than 10%).

Figure 6(ii) shows the impact of a $\pm 10\%$ change in the coefficient a and c of the developing-flow modification factor. This change has led to a variation similar to that observed for the change of the developing-flow modification factor. The impact of varying the coefficient a in the heat-flux-based factor is much smaller than that produced by a change of the coefficient c in the wall-temperature-based factor (4% for the former case as compared to 12% for the latter).

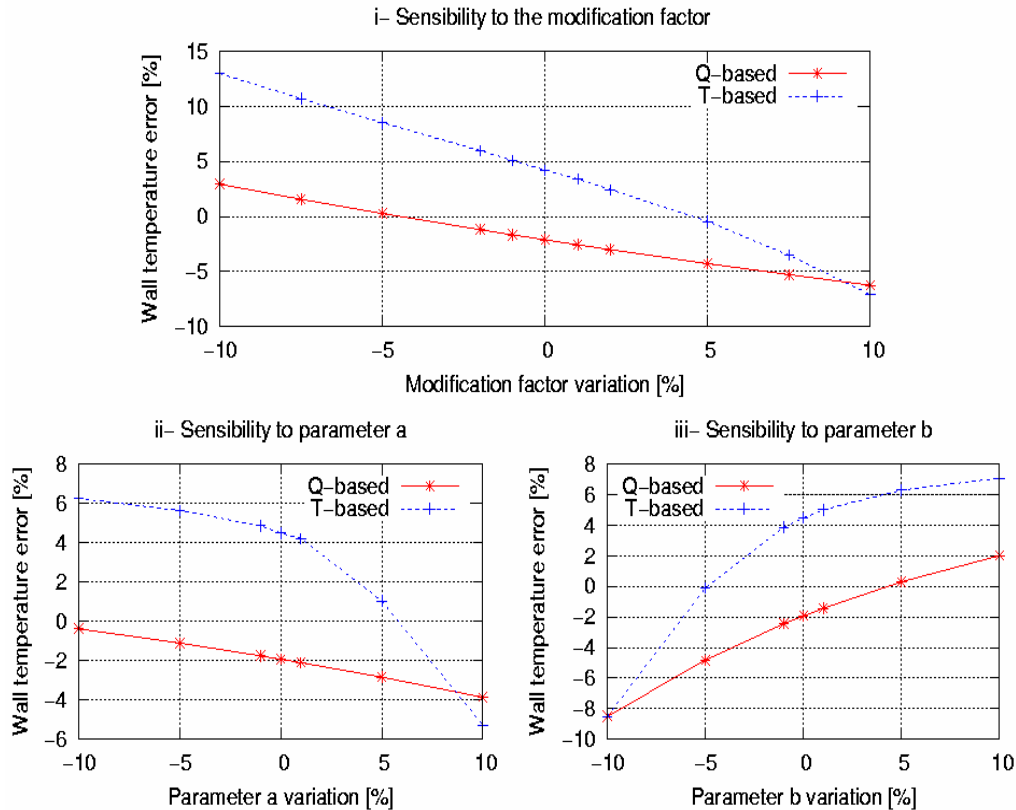


Figure 6: Sensitivity of (i) developing-flow modification factor, and coefficients (ii) a and c , (iii) b on wall-temperature prediction error.

Figure 6(iii) shows the impact of a $\pm 10\%$ change in the coefficient b of the developing-flow modification factor. An augmentation of this coefficient increases the wall-temperature prediction error. The impact of varying the exponent value on prediction error is relatively similar between the heat-flux-based and the wall-temperature-based correlation (i.e., 10% as compared to 15% respectively.)

4.4 Thermal radiation

In general, heat transfer by radiation is relatively small for high-quality post-dryout conditions (often referred as the dispersed-flow film-boiling regime) and therefore, has not been included in the present models. A confirmatory exercise has however been performed in order to determine the impact of thermal radiation on the wall-temperature predictions. As a simplification, an inverted annular film boiling regime was assumed and the heat transfer by radiation is assumed to take place in an annulus-type configuration with the heated wall as the outer surface and the idealized-liquid core at the center. The surfaces are separated by a vapour film having a surface emissivity calculated using the method given in: Leckner [9]. The emissivity of the heated surface depends on both the material and the surface temperature and the emissivity of the water is assumed to be 0.775. Finally, the vapor film temperature was taken as the average of the fluid and wall temperature.

Table 2 shows the maximum ratio of the radiation heat flux to the total heat flux, $(q_{rad}/q_{tot})_{max}$, and the average of the same ratio under post-dryout conditions, $\langle q_{rad}/q_{tot} \rangle_{PDO}$. The maximum impact of the radiation component is about 3% on the heat flux and only about 1% for the average. Including thermal radiation has resulted in a change of less than 0.2% of the predicted wall temperature. Thus, these calculations confirm that for the range of flow conditions studied, the radiation heat transfer has a negligible impact on the post-dryout wall temperature.

Table 2: Impact of thermal radiation on post-dryout temperature predictions

	$(q_{rad}/q_{tot})_{max}$	$\langle q_{rad}/q_{tot} \rangle_{PDO}$	$\langle errT_w \rangle$
Heat-Flux-Based Method	2.73 %	0.89 %	0.07 %
Wall-Temperature-Based Method	2.80 %	1.01 %	0.21 %

5. Conclusions

Two different correlations (i.e., heat-flux and wall-temperature-based correlations) for predicting the post-dryout heat-transfer coefficient have been assessed against a set of experimental data on surface temperatures obtained with a uniformly heated tube. Both correlations provide reasonable wall temperature predictions with an overall average error of -2.1% for the heat-flux-based correlation and of 4.2% for the temperature-based correlation.

The heat-flux-based correlation provides slightly better prediction accuracy and follows the experimental trends observed in the developing-flow region closer than the wall-temperature-based correlation. The prediction accuracy of the post-dryout wall temperature is less sensitive to the variation of the heat-flux-based developing-flow factor than to the variation of the wall-temperature-based factor.

Within the range of flow conditions covered by this work, the impact of the radiation heat transfer on the post-dryout surface-temperature seems to be quite small.

6. References

- [1] Girard, R., Hanna, B. and Leung, L.K.H., "CATHENA New Post-Dryout Heat Transfer Methodology", Proc. 6th Int. Conf. on Simulation Methods in Nuclear Engineering, Montréal, Québec, Canada, October 12-15, 2004.
- [2] Leung, L.K.H., Groeneveld, D.C. and Cheng, S.C., "Separate Effects on Film-Boiling Heat Transfer", Proc. 12th Int. Heat Transfer Conference, Grenoble, France, Aug. 18-23, 2002, pp. 267-272.
- [3] Guo, Y. and Leung, L.K.H., "Correlations for Developing Film Boiling Effect in Tubes", Proc. 11th Topical Meeting on Nuclear Reactor Thermal-Hydraulics (NURETH-11), Avignon, France, Oct. 2-6, 2005.
- [4] Groeneveld, D.C., Leung, L.K.H., Guo, Y., Vasic, A., El Nakla, M., Peng, S.W., Yang, J. and Cheng, S.C., "Look-Up Tables for Predicting CHF and Film-Boiling Heat Transfer:

- Past, Present and Future”, Proc. 10th Topical Meeting on Nuclear Reactor Thermal-Hydraulic, Seoul, Korea, Oct. 3-9, 2003.
- [5] Chen, J.C., “A Correlation for Boiling Heat Transfer to Saturated Fluids in Convective Flow”, Paper ASME 63-HT-34, 1963.
- [6] Becker, K.M., Ling, C.H., Heelberg, S. and Strand, G., “An experimental investigation of post-dryout heat transfer”, KTH-NEL-33, Sweden, 1983.
- [7] Bennett, A.W., Hewitt, G.F., Kearsy, H.A. and Keays, R.K.F. “Heat transfer to steam-water mixtures flowing in uniformly heated tubes in which the critical heat flux has been exceeded”, AERE-R-5373, 1967.
- [8] Groeneveld, D.C., Leung, L.K.H., Kirillov, P.L., Bobkov, V.P., Smogalev, I.P., Vinogradov, V.N., Huang, X.C. and Royer, E., “The 1995 Look-Up Table for Critical Heat Flux in Tubes”, Nuclear Engineering and Design, Vol. 163, pp. 1-23, 1996.
- [9] Leckner, B., “Spectral and Total Emissivity of Water Vapor and Carbon Dioxide”, Combustion and Flame, Vol. 19, pp. 22-48, 1972.

Nomenclature

Bo	Boiling number
h	Heat transfer coefficient (W/m^2K)
G	Mass flux (kg/m^2s)
H_{fg}	Latent heat of vaporization (J/kg)
K_{dev}	Modification factor accounting for the developing flow
LUT	Look-up table
P	Power (kW)
p	Pressure (kPa)
q	Heat flux (kW/m^2)
T	Temperature ($^{\circ}C$ or K)
x	Thermodynamic quality

Subscripts:

CHF	Critical heat flux
DO	dryout
FD	Fully developed
In	Inlet
Max	Maximum
NB	Nucleate boiling
PDO	Post-dryout
Sat	Saturation
W	Wall

Acknowledgement

The principal author of this paper, E.-L. Pelletier, would like to thank Hydro-Québec and the École Polytechnique de Montréal for providing the financial support for carrying out this study.